Rationalizing Inter- and Intracrystal Heterogeneities in Dealuminated Acid Mordenite Zeolites by Stimulated Raman Scattering Microscopy Correlated with Super-resolution Fluorescence Microscopy

Kuan-Lin Liu,[,†,§], Alexey V. Kubarev,[‡,§] Jordi Van Loon,[‡] Hiroshi Uji-i,[†] Dirk E. De Vos,[‡] Johan Hofkens,[†] Maarten B.J. Roeffaers,[*,‡]*

[†]Department of Chemistry, Faculty of Sciences, KU Leuven, 3001 Heverlee, Belgium.

[‡]Centre for Surface Chemistry and Catalysis, Faculty of Bioscience Engineering, KU Leuven, 3001 Heverlee, Belgium.

*Address correspondence to maarten.roeffaers@biw.kuleuven.be (M.B.J.R.) and d927429@alumni.nthu.edu.tw (K.-L.L.).

[§]These authors contributed equally to this work.

KEYWORDS. dealumination; mordenite; single-molecule microscopy; stimulated Raman scattering; super-resolution fluorescence microscopy; Raman microscopy.

Quantification of intracrystal reactivity distribution from NASCA experiments. In order to quantify the inter- and intracrystal heterogeneity reactivity maps containing the localized reaction events for 500 x 500 x 800 nm^3 voxels were reconstructed; the effective thickness of the observed layer is assumed to be 800 nm. The histogram, showing the reactivity distribution, was fitted with Lorentzian curves which give an indication of the number of zones within the crystals which show a distinct catalytic activity. The peak location corresponds to the most often observed reaction rate in the region, whereas FWHM of the peak reports on the degree of heterogeneity in that region. Binned NASCA images, histograms and results of fitting are presented in the Fig. 2 of the main text. The used fitting parameters are summarized in Table S1.

The resolution of NASCA microscopy that can be obtained with current experimental conditions is typically around 20 nm. However, for a detailed statistical analysis large amount of turnovers per voxel is required to clearly deconvolute individual activity peaks in the histogram. Therefore, we decided to use a larger voxel size than the minimal one allowed by the precision of NASCA microscopy.

Table S1. Obtained peak parameters for fitting the histograms in Fig. 2 A-E and displayed in Fig. 2 F-J.

Sample (histogram)	Peak number	Location, ($M \cdot s^{-1} \cdot 10^{-10}$)	Relative Area	FWHM, ($M \cdot s^{-1} \cdot 10^{-10}$)
SP-MOR (2F)	0	0	0.83±0.01	0.65±0.01
	1	2.6±0.1	0.17±0.02	2.5±0.3
SD-MOR (2G)	0	16.6±0.4	1.00	13±1
MD-MOR (2H)	0	0	0.71±0.02	1.24±0.02
	1	2.6±0.6	0.29±0.04	8.3±0.9
MD-MOR (2I)	0	4.3±0.1	0.61±0.02	9.1±0.4
	1	95±3	0.39±0.04	51±8
MD-MOR (2J)	0	2.3±0.2	0.09±0.02	2.3±0.9
	1	24±1	0.91±0.08	29±3

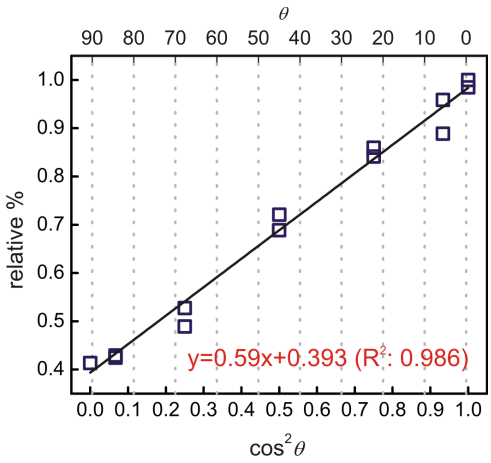

Figure S1. Linear relationship between $\cos^2\theta$ and relative SRS response of C≡N stretch; θ is the angle between laser polarization and crystallographic *b*-axis; the slope and intercept indicate the contributions from anisotropic and isotropic terms, respectively.

Quantification of adsorbed CD_3CN density.

For spontaneous Raman measurement, the procedures of calculating orentiation independent spectrum for a system of uniaxial symmetry have been established. Using the coordinate system given in Fig. S2 the orientation independent spectrum can be obtained from a linear combination of four polarized Raman measurements.[1,2]

$$I^{iso}(3+6R) = I_{bb} + 2I_{cc} + 2I_{ca} + 4I_{bc} \quad \text{(S1)}$$

where I_{ij} indicates the Raman intensity ($I_{ij} = I_{ji}$) measured with incident and scattered photons polarized parallel to the *i* and *j*-directions, respectively; *R* is the Raman depolarization ratio evaluated from an isotropic sample; in this case liquid CD_3CN.[2] Because we are only interested in the C≡N vibration, the depolarization ratio of I_{bb} (R_1) and I_{cc} terms (R_2) can be introduced into equation (S1).

$$R_1 = \frac{I_{bc}}{I_{bb}}, \quad \text{(S2)}$$

$$R_2 = \frac{I_{ca}}{I_{cc}}, \quad \text{(S3)}$$

and thus

$$I^{iso}(3+6R) = I_{bb}(1+4R_1) + 2I_{cc}(1+R_2) \quad \text{(S4)}$$

When performing measurement on a microscope, however, the number of scattering intensities, I_{ij}^{μ} (μ denotes the Raman signal measured using an optical microscope), that can be measured is limited; the four Raman intensities I_{bb}, I_{cc}, I_{ca}, and I_{cb}, can be evaluated by:[3,4]

$$I_{bb} = \frac{1}{AC_0}(I^{\mu}_{bb} - \frac{B}{A+B} I^{\mu}_{bc}), \quad \text{(S5)}$$

$$I_{cc} = \frac{1}{AC_0}(I^{\mu}_{cc} - I^{\mu}_{cb} + \frac{A}{A+B} I^{\mu}_{bc}), \quad \text{(S6)}$$

$$I_{cb} = \frac{I^{\mu}_{bc}}{C_0(A+B)}, \quad \text{(S7)}$$

$$I_{ca} = \frac{1}{BC_0}(I^{\mu}_{cb} - \frac{A}{A+B} I^{\mu}_{bc}), \quad \text{(S8)}$$

with

$$A = \pi^2(\frac{4}{3} - \cos\theta_m - \frac{1}{3}\cos^3\theta_m), \quad \text{(S9)}$$

and

$$B = 2\pi^2(\frac{2}{3} - \cos\theta_m + \frac{1}{3}\cos^3\theta_m) \quad \text{(S10)}$$

where A and B account for the collection of the Raman scattering with an objective of given numerical aperture (NA); C_0 is related to the energy distribution of incident electric field at the focal plane; θ_m is the half angle of NA. The depolarization ratio *R* can be evaluated from the experimental depolarization ratio obtained by microscopy R^{μ}:

$$R^{\mu} = \frac{(A+B)R}{A+BR} \quad \text{(S11)}$$

The relationship between normal Raman intensity and SRS response is given by:[5]

$$I_{ij}^{\mu} = \kappa I_{kl}^{SRS} \tag{S12}$$

where κ is the proportionality coefficient, and a constant κ value is assumed for different configurations of laser polarization. The depolarization ratio (R^{μ}) of the C≡N stretch for liquid CD_3CN is determined with the SRS setup by using parallel and perpendicular polarizations between pump and Stokes beams (Fig. S3A).[6] The obtained depolarization ratio R is 0.04 with a NA=1.05 objective; a low value typical for A1 mode vibrations. $I_{bb}^{SRS}, I_{cc}^{SRS}, I_{bc}^{SRS}$, and I_{cb}^{SRS} are measured for CD_3CN adsorbed in SP-MOR crystals (Fig. S3B). R_1 and R_2 are 0.06 and 0.04, respectively, evaluated by equation (S2), (S3), and (S5)–(S8). By rearranging (S5)–(S8), I_{bb} and I_{cc} can be obtained by

$$I_{bb} = \frac{I_{bb}^{\mu}}{C_0(A + BR_1)} = \frac{\kappa I_{bb}^{SRS}}{C_0(A + BR_1)}, \tag{S13}$$

$$I_{cc} = \frac{I_{cc}^{\mu}}{C_0(A + BR_2)} = \frac{\kappa I_{cc}^{SRS}}{C_0(A + BR_2)}. \tag{S14}$$

By substitution of (S13) and (S14) and of numerical values of A, B, R, R_1, and R_2 into equation (S4), the orientation independent spectrum for adsorbed CD_3CN (I_{ad,CD_3CN}^{iso}) can be calculated by

$$I_{ad,CD_3CN}^{iso} = \frac{\kappa}{\pi^2 C_0}\left(0.58 I_{bb}^{SRS} + 0.98 I_{cc}^{SRS}\right) \tag{S15}$$

On the other hand, for liquid CD_3CN, $I_{CD_3CN}^{iso} = I_{zz}$, and thus

$$I_{CD_3CN}^{iso} = \frac{I_{zz}^{\mu}}{C_0(A + BR)} = \frac{\kappa I_{zz}^{SRS}}{C_0(A + BR)} = \frac{\kappa}{\pi^2 C_0} 1.54 I_{zz}^{SRS}. \tag{S16}$$

where I_{zz}^{SRS} represents the SRS response recorded with pump and Stokes beams polarized along the laboratory *z*-axis. Assuming a similar Raman scattering cross-section, the density of adsorbed CD_3CN can be evaluated by comparing its integrated C≡N peak intensity (S15) to that of liquid CD_3CN (S16) with known density (10.8 nm^{-3}). Note that the uniaxial symmetry is maintained after dealumination (Fig. 4), equation (S15) and (S16) are still valid for the quantification of site density. Similarly, the density map can be reconstructed using (S15) *via* a linear combination of two chemical mappings, at the peak of the C≡N stretch, along crystallographic *b*- and *c*-axes, respectively. The resulting intensity map is orientation independent, assuming constant bandwidth, and after laser power normalization the scale is calibrated with that of liquid CD_3CN (S16).

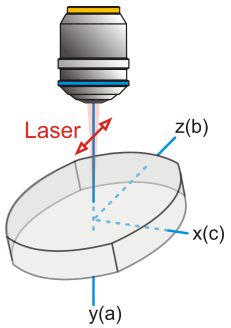

Figure S2 Schematic drawing of laboratory and crystallographic axes (latter shown between brackets); laboratory *z* and *x*-axes are aligned to crystallographic *b* and *c* (or *a*) axes by rotating the crystals before the measurement.

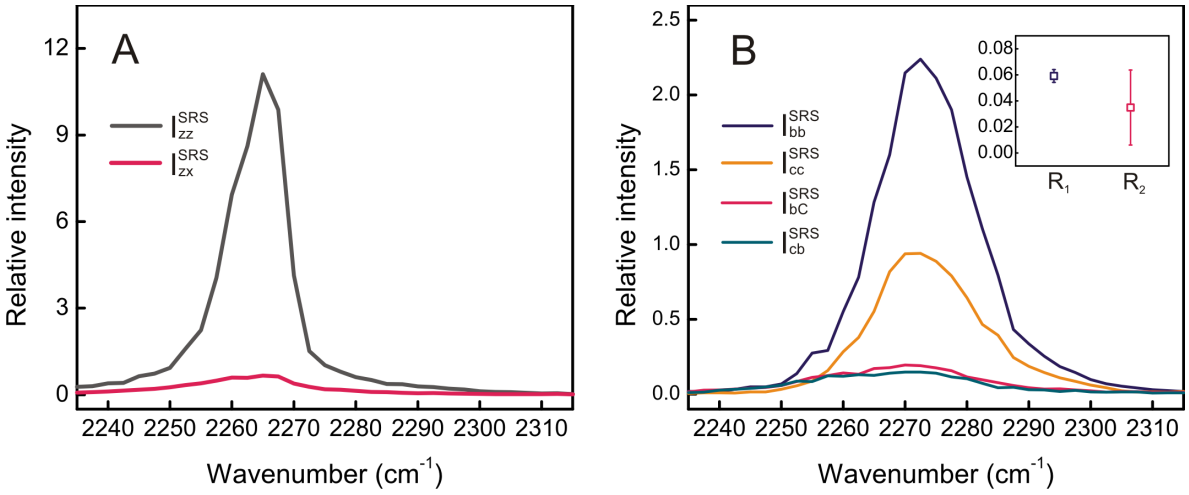

Figure S3. SRS response in the C≡N stretch region of liquid CD_3CN (A) and CD_3CN adsorbed in SP-MOR (B), averaged within the whole crystal, measured with different configurations of laser polarization; inset shows the depolarization ratios R_1 and R_2.

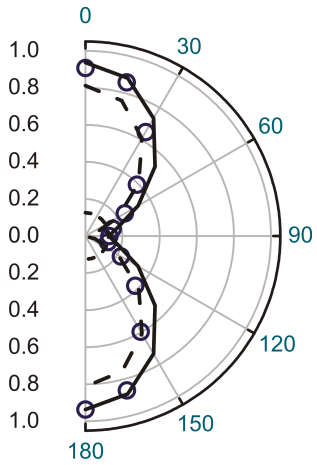

Figure S4. Polar plot of C≡N stretch (2267 cm^{-1}) recorded at the edge of an early dealuminated MD-MOR crystal, where the acid sites in main channels have been preferentially removed.

Quantification of acid site density in main channel and side pocket.

Since the SRS response of C≡N vibration for CD_3CN adsorbed side pockets ($I_{bb}^{SRS} - I_{cc}^{SRS}$) and main channels (I_{cc}^{SRS}) possess a uniaxial (a $\cos^2\theta$ function, θ is the angle between laser polarization and crystallographic *b*-axis) and isotropic symmetry, respectively, their orientation independent spectra can be calculated by substituting individual SRS signal into S15 and S16. Noted the $I_{bb}^{SRS} - I_{cc}^{SRS}$ spectrum approaches maximum and zero with lasers polarized in crystallographic *b*- and *c*-axes, respectively. We thus obtain

$$I_{\text{side pocket}}^{\text{iso}} = \frac{\kappa}{\pi^2 C_0}\left[0.58(I_{bb}^{SRS} - I_{cc}^{SRS})\right], \quad \text{(S17)}$$

$$I_{\text{main channel}}^{\text{iso}} = \frac{\kappa}{\pi^2 C_0} 1.54 I_{cc}^{SRS}. \quad \text{(S18)}$$

The ratio of acid site in side pocket to main channel can be obtained by comparing the integrated intensity of (S17) to that of (S18).

Among SP-MOR crystals the ratio is 0.37±0.05, and is almost a constant within single crystal. However, for MD-MOR samples at early and intermediate stage of dealumination the ratio increases to 0.4–0.5 and 0.7–1.3 at the center and edge of the crystal, respectively, showing the acid sites in the main channel are removed preferentially. For MD-MOR at a late stage of dealumination and for SD-MOR the ratio is 1.3–1.8; this is independent of the position inside a single crystal. Note that CD_3CN adsorbed in the side pocket might possess some orientational freedom resulting in a slight misalignment between the crystallographic *b*-axis and laboratory *z*-axis, which both could result in a slight underestimation of the acid site density in the side pocket; *e.g.* for a C≡N bond oriented at an average angle of 10° with respect to crystallographic *b*-axis the ratio of acid site in side pocket vs. main channel would only increase from 0.37 to 0.40 *i.e.* about 8% difference

Spontaneous Raman measurements. Spontaneous Raman measurements on some H-MOR were performed to validate the SRS spectra. CD_3CN/SP-MOR, PhCN/MD-MOR, and PhCN/SD-MOR samples are selected because of their favorable spontaneous Raman signal. Spontaneous Raman spectra were recorded with an inverted confocal Raman microscope (Ti-U, Nikon). The 632.8 nm line from a He–Ne laser (Research Electro-Optics) was used as the excitation source. Excitation polarization was converted to circular by a quarter-wave plate. The laser beam was guided through a dichroic mirror (Chroma Technology, z633rdc) to the objective and focused onto the center of each crystal with a 60x0.95 NA air objective (Nikon). The backward Raman

scattering was collected by the same objective and passed through a 100-μm confocal pinhole, filtered by a long-pass filter (Chroma Technology, HQ645LP), and directed into a monochromator (HORIBA, iHR320). The signal was dispersed with a 600 grooves/mm grating (Andor Technology) and detected by a CCD camera (Newton, Andor Technology). Typical integration time for each crystal was 5 minutes.

Figure S5A presents spontaneous Raman spectra of CD_3CN adsorbed in SP-MOR; the C≡N stretch shifts to 2274.6±0.7 cm^{-1} which resembles the wavenumbers obtained with SRS microscopy. Figures S5B,C show the spontaneous Raman spectra of PhCN adsorbed in MD- and SD-MOR, respectively. Similar spectral profiles with two C≡N vibrational frequencies are observed for PhCN, which are 2238.1±0.7 and 2247.8±1.6 cm^{-1}, respectively. The spontaneous Raman measurements validate the approach, SRS microscopy in combination with nitrile probe, employed in this study.

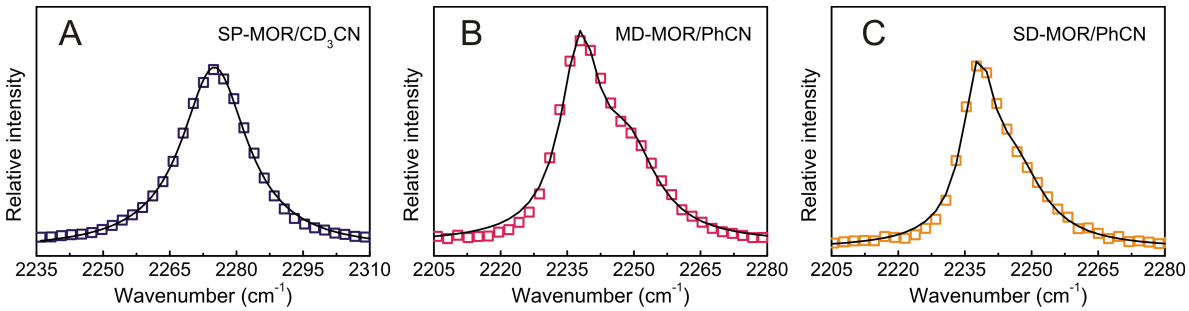

Figure S5 (**A**–**C**) Spontaneous Raman measurement of SP-MOR/CD_3CN (**A**), MD-MOR/PhCN (**B**), and SD-MOR/PhCN (**C**); experimental data of SP-MOR and MD-, SD-MOR are fitted by a single Lorentzian curves and a sum of two Lorentzian curves (solid line), respectively.

References:

1. Tanaka, M.; Young, R. J. Review Polarised Raman Spectroscopy for the Study of Molecular Orientation Distributions in Polymers. *J. Mater. Sci.* **2006**, *41*, 963–991.

2. Frisk, S.; Ikeda, R. M.; Chase, D. B.; Rabolt, J. F. Rotational Invariants for Polarized Raman Spectroscopy. *Appl. Spectrosc.* **2003**, *57*, 1053–1057.

3. Lefèvre, T.; Rousseau, M.-E.; Pézolet, M. Orientation-Insensitive Spectra for Raman Microspectroscopy. *Appl. Spectrosc.* **2006**, *60*, 841–846.

4. Sourisseau, C. Polarization measurements in macro- and micro-Raman Spectroscopies: Molecular Orientations in Thin Films and Aazo-Dye Containing Polymer Systems. *Chem. Rev.* **2004**, *104*, 3851–3892.

5. Levenson, M. D.; Kano, S. S. *Introduction to Nonlinear Laser Spectroscopy* (Academic Press INC., London 1988).

6. Munhoz, F.; Brustlein, S.; Hostein, R.; Berto, P.; Brasselet, S.; Rigneault, H. Polarization Resolved Stimulated Raman Scattering Probing Depolarization Ratios of Liquids. *J. Raman. Spectrosc.* **2012**, *43*, 419–424.